

case-cohort design is suitable for cross-sectional analyses,⁴⁶ such as assessing allele frequencies and Hardy-Weinberg equilibrium (an important but not essential assumption for association studies^{60,61}). Finally, we note that if the only impact of a gene is to modify the effect of environmental exposure, a main effect of genotype/haplotype may not be required in the model.⁶² Alternatively, it is conceivable that a gene evidencing both a direct effect on outcome and modification of risk of an environmental factor might not necessarily exert both effects according to the same genomic model if they involve separate mechanisms. A number of further issues are discussed in detail in two recent publications.^{63,64}

In conclusion, for studying interactions with an exposure variable, we recommend that case-cohort studies be conducted based on exposure-stratified random sampling when exposure can be ascertained in the entire cohort. When stratification is not necessary, the exact PsL with asymptotic variance estimates may be used and the most flexible implementation is to be found in the Epicure software. With stratified case-cohort data, we recommend the score-unbiased method III (the swapper method) of Borgan *et al.*,²⁹ with variances estimated using the asymptotic method. Stratified data may be analysed using the SAS macros of Langholz and Jiao¹⁸ or the S-plus function provided here (Supplementary Appendix A1 available at *IJE* online). Further work is needed to extend existing software for stratified case-cohort data to allow fitting of risk models that are more general than the standard proportional hazards model.

Supplementary Data

Supplementary Data are available at *IJE* online.

Funding

This work was supported by the Radiation Effects Research Foundation (RERF), Hiroshima and Nagasaki, Japan, a private, non-profit foundation funded by the Japanese Ministry of Health, Labour and Welfare (MHLW) and the U.S. Department of Energy (DOE), the latter in part through the National Academy of Sciences [RERF Research Protocol RP 4-04]; the Ministry of Education, Culture, Sports, Science and Technology of Japan [Grant-in-Aid for Scientific Research (B) 21390199]; and the Ministry of Health, Labour and Welfare of Japan [Grant-in-Aid for Cancer Research 22090501].

Acknowledgements

The authors express sincere gratitude to Professor Bryan Langholz for assistance with the swapper method for stratified case-cohort data and to Dr Robert Abbott for guidance on the logistic regression approximation to Cox regression (both have provided their consent to be so acknowledged).

Conflict of interest: D.L.P. was the principal developer of the Epicure software, which is now owned by Risk Sciences International (RSI). Although he no longer owns the software, there is a possibility he might receive royalties on some future sales of the software.

KEY MESSAGE

- We summarize the literature on case-cohort design and analysis and make recommendations regarding its implementation for studies of gene-environment interaction. Stratified, rather than simple, random sampling should be preferred when exposure information exists for the entire cohort. The current state of relevant software is reviewed, and needs are identified for further development of software tools that allow fitting general, flexible risk models. Given that the subcohort can be used for assessment of population parameters, such as allele frequencies and Hardy-Weinberg equilibrium, the case-cohort design is well suited to molecular epidemiological research.

References

- 1 Preston DL, Ron E, Tokuoka S *et al.* Solid cancer incidence in atomic bomb survivors: 1958-1998. *Radiat Res* 2007;**168**:1-64.
- 2 Yamada M, Wong FL, Fujiwara S, Akahoshi M, Suzuki G. Noncancer disease incidence in atomic bomb survivors, 1958-1998. *Radiat Res* 2004;**161**:622-32.
- 3 Hayashi T, Kusunoki Y, Kyoizumi S *et al.* Relationship between cancer development and genetic polymorphisms among A-bomb survivors, focusing on immune-related genes. Research Protocol 4-04. Hiroshima, Japan: Radiation Effects Research Foundation, 2004; http://www.rerf.jp/programs/rparchiv_c/rp04-04.htm (5 July 2012, date last accessed).
- 4 Yoshida K, Nakachi K, Imai K *et al.* Lung cancer susceptibility among atomic bomb survivors in relation to CA repeat number polymorphism of *epidermal growth factor receptor* gene and radiation dose. *Carcinogenesis* 2009;**30**:2037-41.
- 5 Cox DR. Regression models and life tables. *J R Stat Soc Series B* 1972;**34**:187-202.
- 6 Preston DL, Lubin JH, Pierce DA, McConney ME. *Epicure Users Guide*. Seattle: Hirosoft International Corporation, 1993.

- ⁷ Breslow NE, Day NE. *Statistical Methods in Cancer Research, Volume II – The Design and Analysis of Cohort Studies*. Lyon: International Agency for Research on Cancer, 1987.
- ⁸ Langholz B, Borgan Ø. Counter-matching: a stratified nested case-control sampling method. *Biometrika* 1995; **82**:69–79.
- ⁹ Cologne J, Langholz B. Selecting controls for assessing interaction in nested case-control studies. *J Epidemiol* 2003; **13**:193–202.
- ¹⁰ Cologne JB, Sharp GB, Neriishi K, Verkasalo PK, Land CE, Nakachi K. Improving the efficiency of nested case-control studies of interaction by selecting controls using counter matching on exposure. *Int J Epidemiol* 2004; **33**:485–92.
- ¹¹ Prentice RL. A case-cohort design for epidemiologic cohort studies and disease prevention trials. *Biometrika* 1986; **73**:1–11.
- ¹² Langholz B, Thomas DC. Nested case-control and case-cohort methods of sampling from a cohort: a critical comparison. *Am J Epidemiol* 1990; **131**:169–76.
- ¹³ Wacholder S. Practical considerations in choosing between the case-cohort and nested case-control designs. *Epidemiology* 1991; **2**:155–58.
- ¹⁴ Volovics A, van den Brandt PA. Methods for the analysis of case-cohort studies. *Biom J* 1997; **39**:195–214.
- ¹⁵ Barlow WE, Ichikawa L, Rosner D, Izumi S. Analysis of case-cohort designs. *J Clin Epidemiol* 1999; **52**:1165–72.
- ¹⁶ Zeng D, Lin DY, Avery CL, North KE, Bray MS. Efficient semiparametric estimation of haplotype-disease associations in case-cohort and nested case-control studies. *Biostatistics* 2006; **7**:486–502.
- ¹⁷ Self SG, Prentice RL. Asymptotic distribution theory and efficiency results for case-cohort studies. *Ann Stat* 1988; **16**:64–81.
- ¹⁸ Langholz B, Jiao J. Computational methods for case-cohort studies. *Comp Statist Data Anal* 2007; **51**:3737–48.
- ¹⁹ Therneau TM, Li H. Computing the Cox model for case cohort designs. *Lifetime Data Anal* 1999; **5**:99–112.
- ²⁰ Lin DY, Ying Z. Cox regression with incomplete covariate measurements. *J Am Stat Assoc* 1993; **88**:1341–49.
- ²¹ Chen K, Lo SH. Case-cohort and case-control analysis with Cox's model. *Biometrika* 1999; **86**:755–64.
- ²² Kulich M, Lin DY. Improving the efficiency of relative-risk estimation in case-cohort studies. *J Am Stat Assoc* 2004; **99**:832–44.
- ²³ Scheike TH, Martinussen T. Maximum likelihood estimation for Cox's regression model under case-cohort sampling. *Scand J Stat* 2004; **31**:283–93.
- ²⁴ Breslow NE, Lumley T, Ballantyne CM, Chambless LE, Kulich M. Using the whole cohort in the analysis of case-cohort data. *Am J Epidemiol* 2009; **169**:1398–405.
- ²⁵ Chen K. Generalized case-cohort sampling. *J R Stat Soc Series B* 2001; **63**:791–809.
- ²⁶ Onland-Moret NC, van der ADL, van der Schouw YT *et al*. Analysis of case-cohort data: a comparison of different methods. *J Clin Epidemiol* 2007; **60**:350–55.
- ²⁷ Kulathinal S, Karvanen J, Saarela O, Kuulasmaa K. Case-cohort design in practice – experiences from the MORGAM Project. *Epidemiol Perspect Innov* 2007; **4**:15.
- ²⁸ Samuelsen SO, Anestad H, Skrondal A. Stratified case-cohort analysis of general cohort sampling designs. *Scand J Stat* 2007; **34**:103–19.
- ²⁹ Borgan Ø, Langholz B, Samuelsen SO, Goldstein L, Pogoda J. Exposure stratified case-cohort designs. *Lifetime Data Anal* 2000; **6**:39–58.
- ³⁰ Breslow N. "cch: Fits proportional hazards regression model to case-cohort data". Function in Therneau T: "Package 'survival': Survival analysis, including penalised likelihood". R package; version 2.36-12, <http://cran.r-project.org/web/packages/survival/survival.pdf>, February 15 2012 (accessed 15 March 2012).
- ³¹ Therneau T. Package 'survival': Survival analysis, including penalised likelihood. R package; version 2.36-12, February 15, 2012, <http://cran.r-project.org/web/packages/survival/survival.pdf> (accessed 15 March 2012).
- ³² Miettinen S. Design options in epidemiologic research: an update. *Scand J Work Environ Health* 1982; **8**(Suppl 1): 7–14.
- ³³ Greenland S. Adjustment of risk ratios in case-base studies (hybrid epidemiologic designs). *Stat Med* 1986; **5**: 579–84.
- ³⁴ Sato T. Estimation of a common risk ratio in stratified case-cohort studies. *Stat Med* 1992; **11**:1599–605.
- ³⁵ Barlow WE. Robust variance estimation for the case-cohort design. *Biometrics* 1994; **50**:1064–72.
- ³⁶ Therneau TM, Grambsch PM. *Modeling Survival Data: Extending the Cox Model*. New York: Springer-Verlag, 2000.
- ³⁷ Wacholder S, Gail MH, Pee D, Brookmeyer R. Alternative variance and efficiency calculations for the case-cohort design. *Biometrika* 1989; **76**:117–23.
- ³⁸ Mark SD, Katki H. Influence function based variance estimation and missing data issues in case-cohort studies. *Lifetime Data Anal* 2001; **7**:331–44.
- ³⁹ Kulich M, Lin DY. Additive hazards regression for case-cohort studies. *Biometrika* 2000; **87**:73–87.
- ⁴⁰ Moger TA, Pawitan Y, Borgan Ø. Case-cohort methods for survival data on families from routine registries. *Stat Med* 2008; **27**:1062–74.
- ⁴¹ Lin DY, Wei LJ. The robust inference for the Cox proportional hazards model. *J Am Stat Assoc* 1989; **84**:1074–78.
- ⁴² Nan B. Efficient estimation for case-cohort studies. *Can J Stat* 2004; **32**:403–19.
- ⁴³ Kupper LL, McMichael AJ, Spirtas R. A hybrid epidemiologic study design useful in estimating relative risk. *J Am Stat Assoc* 1975; **70**:524–28.
- ⁴⁴ Cologne J, Hsu W-L, Abbott RD *et al*. Proportional hazards regression in epidemiologic follow-up studies: an intuitive consideration of primary time scale. *Epidemiology* 2012; **23**:565–73.
- ⁴⁵ Rothman KJ, Greenland S, Lash TL. *Modern Epidemiology*. 3rd edn. Philadelphia: Lippincott Williams & Wilkins, 2008.
- ⁴⁶ Rundle AG, Vineis P, Ahsan H. Design options for molecular epidemiology research within cohort studies. *Cancer Epidemiol Biomarkers Prev* 2005; **14**:1899–907.
- ⁴⁷ Mark SD, Katki HA. Specifying and implementing non-parametric and semiparametric survival estimators in two-stage (nested) cohort studies with missing case data. *J Am Stat Assoc* 2006; **101**:460–71.
- ⁴⁸ Sørensen P, Andersen PK. Competing risks analysis of the case-cohort design. *Biometrika* 2000; **87**:49–59.
- ⁴⁹ Cai J, Zeng D. Power calculation for case-cohort studies with nonrare events. *Biometrics* 2007; **63**:1288–95.
- ⁵⁰ Breslow NE, Lumley T, Ballantyne CM, Chambless LE, Kulich M. Improved Horvitz-Thompson estimation of model parameters from two-phase stratified samples: applications in epidemiology. *Stat Biosci* 2009; **1**:32–49.

- ⁵¹ Breslow NE, Chatterjee N. Design and analysis of two-phase studies with binary outcome applied to Wilms tumour prognosis. *Appl Stat* 1999;**48**:457–68.
- ⁵² Whittemore AS. Multistage sampling designs and estimating equations. *J R Stat Soc Series B* 1997;**59**:589–602.
- ⁵³ Robins JM, Rotnitzky A, Zhao LP. Estimation of regression coefficients when some regressors are not always observed. *J Am Stat Assoc* 1994;**89**:846–66.
- ⁵⁴ Kong L, Cai J. Case-cohort analysis with accelerated failure time model. *Biometrics* 2009;**65**:135–42.
- ⁵⁵ Kulathinal S, Arjas E. Bayesian inference from case-cohort data with multiple end-points. *Scand J Stat* 2006;**33**:25–36.
- ⁵⁶ Cornelis MC, Tchetgen EJT, Liang L *et al*. Gene-environment interactions in genome-wide association studies: a comparative study of tests applied to empirical studies of type 2 diabetes. *Am J Epidemiol* 2012;**175**:191–202.
- ⁵⁷ Sinnwell JP, Schaid DJ. Package haplo.stats': Statistical analysis of haplotypes with traits and covariates when linkage phase is ambiguous. *R package*; version 1.5.5, February 25, 2012. <http://cran.r-project.org/web/packages/haplo.stats/haplo.stats.pdf> (accessed 15 March 2012).
- ⁵⁸ Mukherjee B, Ahn J, Gruber SB, Chatterjee N. Testing gene-environment interaction in large-scale case-control association studies: possible choices and comparisons. *Am J Epidemiol* 2012;**175**:177–90.
- ⁵⁹ Mukherjee B, Ahn J, Gruber SB, Chatterjee N. Response to invited commentary "GE-whiz! Ratcheting up gene-environment studies". *Am J Epidemiol* 2012;**175**:208–9.
- ⁶⁰ Trikalinos TA, Salanti G, Khoury MJ, Ioannidis JPA. Impact of violations and deviations in Hardy-Weinberg equilibrium on postulated gene-disease associations. *Am J Epidemiol* 2006;**163**:300–9.
- ⁶¹ Lin DY, Zeng D, Millikan R. Maximum likelihood estimation of haplotype effects and haplotype-environment interactions in association studies. *Genet Epidemiol* 2005;**29**:299–312.
- ⁶² Thomas DC, Lewinger JP, Murcray CE, Gauderman WJ. Invited commentary: GE-whiz! Ratcheting gene-environment studies up to the whole genome and the whole exposome. *Am J Epidemiol* 2012;**175**:203–7.
- ⁶³ Khoury MJ, Wacholder S. Invited commentary: from genome-wide association studies to gene-environment-wide interaction studies—challenges and opportunities. *Am J Epidemiol* 2009;**169**:227–30.
- ⁶⁴ Thomas D. Gene-environment-wide association studies: emerging approaches. *Nat Rev Genet* 2010;**11**:259–72.
- ⁶⁵ Samuelsen SO. *Case-cohort studies: Pre-course 13. Norwegian Epidemiology Conference Tromsø 23–24*. Presentation slides, November, 2005 <http://folk.uio.no/osamuels/casecohort4.pdf> (accessed 15 March 2012).

Compromised hematopoiesis and increased DNA damage following non-lethal ionizing radiation of a human hematopoietic system reconstituted in immunodeficient mice

Changshan Wang¹, Shunsuke Nakamura¹, Motohiko Oshima¹, Makiko Mochizuki-Kashio¹, Yaeko Nakajima-Takagi¹, Mitsujiro Osawa¹, Yoichiro Kusunoki², Seishi Kyoizumi², Kazue Imai², Kei Nakachi² & Atsushi Iwama¹

¹Department of Cellular and Molecular Medicine, Graduate School of Medicine, Chiba University, Chiba, and ²Department of Radiobiology/Molecular Epidemiology, Radiation Effects Research Foundation, Hiroshima, Japan

Abstract

Purpose: Precise understanding of radiation effects is critical to development of new modalities for the prevention and treatment of radiation-induced damage. In this study, we evaluated the effects of non-lethal doses of X-ray irradiation on human hematopoietic stem and progenitor cells (HSPC) reconstituted in NOD/Shi-*scid*, IL2R γ ^{null} (NOG) immunodeficient mice.

Materials and methods: We transplanted cord blood CD34⁺ HSPC into NOG mice irradiated with 2.0 Gy via tail veins. At the 12th week after transplantation, the NOG mice were irradiated with 0, 0.5, 1.0, 2.0, or 4.0 Gy, and the radiation effects on human HSPC *in vivo* were evaluated.

Results: Although a majority of the mice irradiated with 2.0 Gy or more died in 12 weeks after irradiation, the mice that were exposed to 0.5 or 1.0 Gy of irradiation survived and were subjected to analysis. The chimerism of human CD45⁺ hematopoietic cells in peripheral blood and bone marrow (BM) of the recipient mice was reduced in an X-ray dose-dependent manner after irradiation. Percentages of human CD34⁺ HSPC as well as human CD34⁺CD38⁻ HSC in BM similarly declined. CD34⁺CD38⁻ HSC purified from the humanized mice at the 12th week after irradiation showed significantly increased numbers of phosphorylated H2AX (γ H2AX) foci, a marker of DNA breaks, in an X-ray dose-dependent manner. Expression of p16^{INK4A}, a hallmark of aging of HSC, was also detected only in HSPC from irradiated mice.

Conclusions: With further refinement, the humanized mouse model might be effectively used to study the biological effects of non-lethal radiation *in vivo*.

Keywords: Human HSPC; radiation effect; DNA damage; NOG immunodeficient mice

Introduction

Effects of ionizing radiation on human hematopoietic stem and progenitor cells (HSPC) have not been well characterized *in vivo* due to difficulties in bioassays using bone

marrow (BM) samples. In mice, sublethal doses of total-body irradiation (TBI) have been reported to induce hematopoietic stem cells (HSC) senescence accompanied with impaired self-renewal capacity of HSC and upregulated biomarkers of cellular senescence, including p16^{INK4a} (Wang et al. 2006). Furthermore, radiation-induced genomic instability in normal hematopoietic cells has been demonstrated to persist for a prolonged period *in vivo* (Watson et al. 2001). We have also previously reported that genomic effects of irradiation on the murine hematopoietic system persisted *in vivo* for long periods in terms of an increased number of micronucleated reticulocytes in peripheral blood (PB) as an indicator of genomic instability (Hamasaki et al. 2007). In contrast, radiation effects on human HSPC have been evaluated mainly *in vitro* (Rübe et al. 2011). Although human hematopoietic progenitor cells have been evaluated *in vivo* using the human fetus bone transplanted into *scid/scid* (SCID) mice (Kyoizumi et al. 1994), more precise understanding of radiation effects *in vivo* on HSPC is critical to develop new modalities for the prevention and treatment of radiation-induced damage.

In this study, we demonstrate that 0.5 and 1.0 Gy TBI affected the function of human HSC reconstituted in NOG immunodeficient mice. We propose that the humanized mouse model is useful for the evaluation of the radiation effects on human hematopoiesis, particularly in the dose region where long-term effects on the hematopoietic system as well as other organs have been observed among atomic-bomb survivors (Nakachi et al. 2008).

Materials and methods

Transplantation

NOG immunodeficient mice were supplied by the Central Institute for Experimental Animals (Kawasaki, Kanagawa, Japan) and maintained in the Animal Research Facility of the Graduate School of Medicine, Chiba University, in

Correspondence: Prof. Atsushi Iwama, MD, Department of Cellular and Molecular Medicine, Graduate School of Medicine, Chiba University, 1-8-1 Inohana, Chuo-ku, Chiba 260-8670, Japan. Tel: +81 43 226 2187. Fax: +81 43 226 2191. E-mail: aiwama@faculty.chiba-u.jp

(Received 21 June 2012; revised 27 July 2012; accepted 2 September 2012)

accordance with institutional guidelines. This study was approved by the Institutional Review Committees of Chiba University (approval numbers 21-65 and 21-150). Human cord blood (hCB) CD34⁺ cells with a purity of over 95% were purchased from Lonza (Basel, Switzerland). Frozen stock of the CD34⁺ cells were thawed and plated at 5×10^5 cells/well in a six-well plate pre-coated with 25 $\mu\text{g/ml}$ fibronectin fragment CH-296 (Takara Shuzo, Otsu, Shiga, Japan) and cultured in serum-free medium, StemSpan SFEM (Stem Cell Technologies, Vancouver, BC, Canada) in the presence of 100 ng/ml human stem cell factor (SCF) (PeproTech, Rocky Hill, NJ, USA) and 50 ng/ml human thrombopoietin (TPO) (PeproTech) for 16 h. Subsequently, 5×10^4 CD34⁺ cells were injected intravenously into 8-week-old NOG mice which had been irradiated with 2.0 Gy X-ray 2 h before. It has been reported that human HSC are mostly cycling at the early time points post-transplantation in NOG mice, but enter the quiescent state by 18 weeks post-transplantation (Yahata et al. 2011). We assumed that 12 weeks post-transplantation human HSC are well repopulated and substantially quiescent in humanized mice. Therefore, we irradiated mice with the test doses as indicated at the 12th week after transplantation. The same situation was assumed after irradiation. Therefore, we sacrificed mice for analysis at the 12th week after irradiation.

Irradiation

Mice were irradiated on a rotating platform of the Hitachi MBR1520R X-ray machine (150 kV; 20 mA; dose-rate: 1.5 Gy/min; 0.5 mm aluminum and 0.1 mm copper filters). Irradiation doses were verified by performing dosimetry using nanoDot dosimeters (Landauer, Glenwood, IL, USA). For 4 weeks after irradiation, mice were fed with drinking water containing 0.17 mg/ml enrofloxacin.

Flow cytometry

Human cells in the BM and PB of recipient mice were stained with PE-Cy7-conjugated anti-human CD45, APC-conjugated anti-human CD34, PE-conjugated anti-human CD38, and APC-Cy7-conjugated anti-human CD3, PE-conjugated anti-human CD11b, or PE-Cy7-conjugated anti-human CD19 (BD Biosciences, San Jose, CA, USA). They were then analyzed and sorted on a FACS Aria II (BD Biosciences).

Quantitative real-time PCR analysis

Total RNA was isolated using TRIZOL LS solution (Invitrogen, Carlsbad, CA, USA) and reverse transcribed by the ThermoScript RT-PCR system (Invitrogen) with an oligo dT primer. Real-time quantitative PCR was performed with an ABI prism 7300 Thermal Cycler (Applied Biosystems, Foster City, CA, USA) using FastStart Universal Probe Master (Roche Diagnostics, Branchburg, NJ, USA). *GAPDH* expression was used to calculate relative expression levels. Probe numbers and primer sequences were: Probe #65, 5'-AGGTGGGTAGAGGGTCTGC-3' and 5'-TCCAATCCCCTGCAAAC-3' for *p16^{INK4A}*; and probe #25, 5'-ctgactcaacagcagcacc-3' and 5'-tagccaattcgtgtcatacc-3' for *GAPDH*.

Immunostaining of γ H2AX

Cells were incubated in a culture medium drop on slide glasses pre-treated with poly-L-lysine (Sigma, St Louis, MO, USA) for 2 h at 37°C. After fixation with 2% paraformaldehyde, treatment with 0.25% triton X-100, and blocking in 4% sheep serum for 30 min at room temperature, cells were incubated with purified anti-phospho-histone H2AX (Ser139) rabbit polyclonal antibody (Cell Signaling Technology, Danvers, MA, USA) for 12 h at 4°C. The cells were then washed and incubated with Alexa Flour 555-conjugated anti-rabbit IgG goat polyclonal antibody (Invitrogen) for 60 min at room temperature with protection from light. DNA was counterstained with 4',6-diamidino-2-phenylindole (DAPI). Images were taken with a Keyence EZ-9000 fluorescence microscope.

Statistical analysis

The significance tests were performed by nonparametric methods: Jonckheere-Terpstra test for linear trend of percentage changes of human cells in the PB or BM across irradiation doses, and Chi-square test for the association between levels of γ H2AX foci and irradiation dose in a 4×3 contingency table. Kaplan-Meier model was used for the difference of survival rates among mice irradiated with different doses. Statistical analysis was performed using SPSS (version 14.0, SPSS, Chicago, IL, USA).

Results

To evaluate the radiation effects on human HSPC *in vivo*, we transplanted 5×10^4 cord blood CD34⁺ HSPC into NOG mice irradiated with 2.0 Gy via tail veins (Figure 1A). NOG is a mouse strain that exhibits severe immunodeficiency with lack of T, B, and natural killer (NK) cells. It has been reported that the human hematopoietic system can be effectively reconstructed in NOG mice by transplanting human HSC (Ito et al. 2002). At the 12th week after transplantation, the NOG mice showed considerably high chimerism, i.e., the median percentage of human CD45⁺ hematopoietic cells in PB, was 61.5% (range, 37.6–74.4%, $n = 45$). The mice were randomly grouped into five categories and irradiated with 0, 0.5, 1.0, 2.0, or 4.0 Gy for each group (Figure 1A). NOG mice are susceptible to irradiation because of the *scid/scid* background (Fulop and Phillips 1990). Although the 50% lethal dose (LD_{50}) of NOG mice at a single exposure is 3.5 Gy (Ito M, personal communication), the LD_{50} of NOG mice already given prior exposure to 2.0 Gy of X-ray should be lower than 3.5 Gy. As expected, a majority of the mice irradiated with 2.0 Gy or more died within 12 weeks after irradiation (Figure 1B). Therefore, we focused on the mice that were exposed to 0.5 or 1.0 Gy of irradiation in this study.

The chimerism of human hematopoietic cells in PB of the control (non-irradiated) mice was about 50% after an additional 12 weeks (24 weeks in total after transplantation), and during the same period after irradiation the chimerism decreased in a dose-dependent manner while that of mouse hematopoietic cells increased (Figure 2A). Percentage of human CD3⁺ T cells in PB increased at the expense of CD19⁺ B cells and CD11b⁺ myeloid cells during the latter 12 weeks

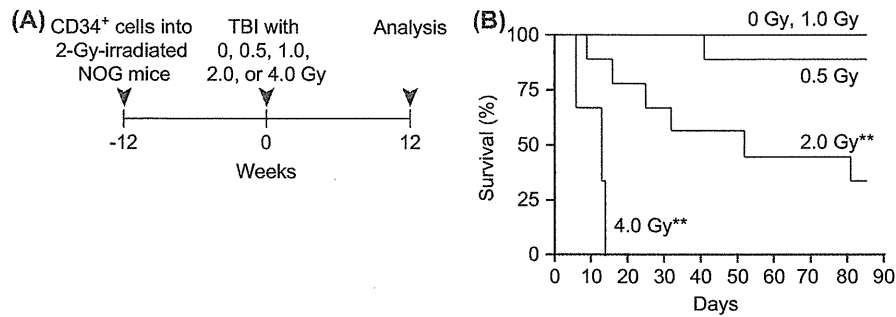


Figure 1. Experimental design and survival of humanized NOG mice after irradiation (A) Schema of experimental strategy. Cord blood CD34⁺ HSPC (5×10^4) were transplanted into 8-week-old NOG mice irradiated with 2.0 Gy via tail veins. At the 12th week after transplantation, the mice were irradiated with 0, 0.5, 1.0, 2.0, or 4.0 Gy. After an additional 12 weeks (24 weeks in total after transplantation), the mice were sacrificed and subjected to detailed analysis. (B) A Kaplan-Meier survival curve of NOG mice after irradiation at doses indicated (0, 0.5, 1.0, 2.0, and 4.0 Gy; $n = 9$ in each dose group). 5×10^4 CD34⁺ cells were injected intravenously into 8-week-old NOG mice irradiated with 2.0 Gy of X-rays. At the 12th week after transplantation, the chimerism of human CD45⁺ hematopoietic cells in PB mononuclear cells (mouse CD45⁺ cells plus human CD45⁺ cells) was analyzed. Then, the mice were randomly grouped into five test radiation dose categories (0, 0.5, 1.0, 2.0, and 4.0 Gy). ** $P < 0.01$.

and irradiation enhanced these changes although they were not statistically significant (Figure 2B). Likewise, X-irradiation reduced the chimerism of human CD45⁺ hematopoietic cells in BM as well as their absolute numbers in a dose-dependent manner (Figure 3A and B). Instead those of mouse hematopoietic cells in BM increased (Figure 3C). Percentages of human CD34⁺ HSPC and human CD34⁺CD38⁻ HSC in CD45⁺ human hematopoietic cells as well as their absolute numbers similarly declined (Figure 3B).

DNA damage is intimately linked to stem cell aging. Heritable DNA damage accrued in stem cells leads to stem cell senescence or apoptosis, which over time can lead to the shrinkage of the stem-cell pool and reduced regenerative capacity of stem cells (Rossi et al. 2008, Yahata et al. 2011). To evaluate the

status of genomic damage in irradiated HSC, we next purified CD34⁺CD38⁻ HSC from the humanized mice at the 12th week after irradiation and determined the phosphorylation status of H2AX at Ser139, γ H2AX, a marker of DNA breaks (Srivastava et al. 2009). Even the freshly isolated CD34⁺CD38⁻ cell fraction from human CB occasionally had γ H2AX foci, and a similar cell fraction purified from non-irradiated humanized mice at 24 weeks post-transplantation also possessed such loci but included more cells with multiple γ H2AX foci. Of note, compared to human HSC isolated from non-irradiated mice, those from irradiated mice showed significantly increased numbers of γ H2AX foci (Figure 4A). We further examined the expression of *p16^{INK4A}*, a hallmark of aging of HSC (Janzen et al. 2006). Because of the limited number of CD34⁺CD38⁻ HSC

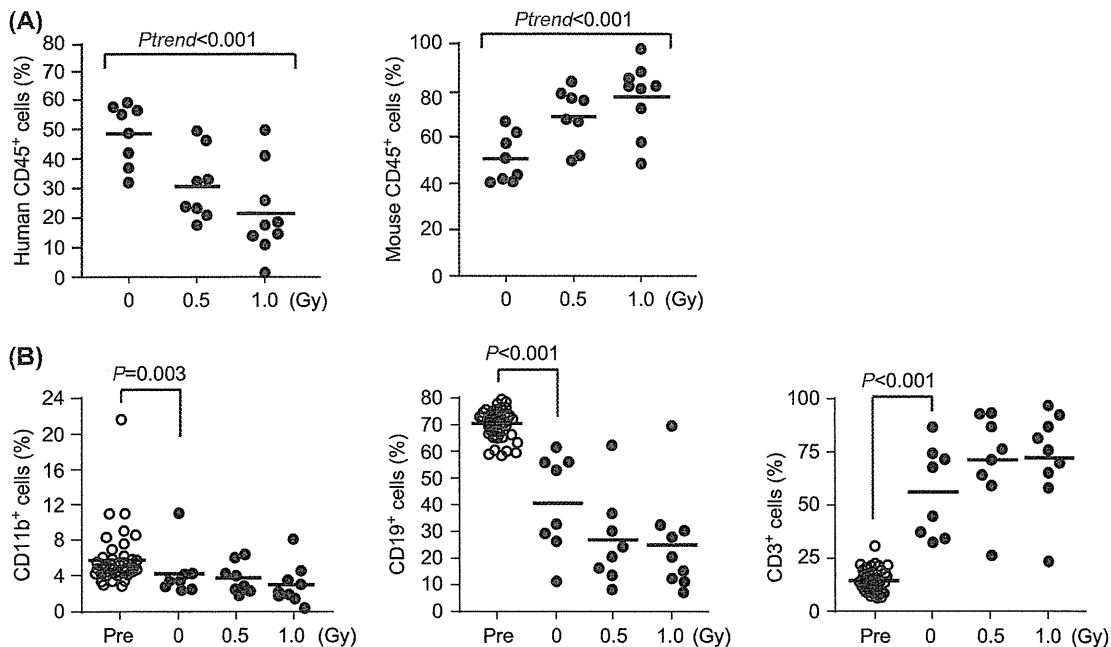


Figure 2. Contribution of human hematopoietic cells in PB of humanized mice following total-body irradiation (A) Changes in chimerism of human hematopoietic cells in PB after irradiation. At the 12th week after irradiation, the chimerism of CD45⁺ human (left panel) and mouse (right panel) hematopoietic cells in PB of survived mice was analyzed, being indicated by dots ($n = 8$ or 9 in each dose group). Median values are indicated by bars. (B) The percentages of CD11b⁺ myeloid cells, CD19⁺ B cells, and CD3⁺ T cells in CD45⁺ human hematopoietic cells in PB of NOG mice just before the irradiation (Pre) and at 12 weeks after irradiation.

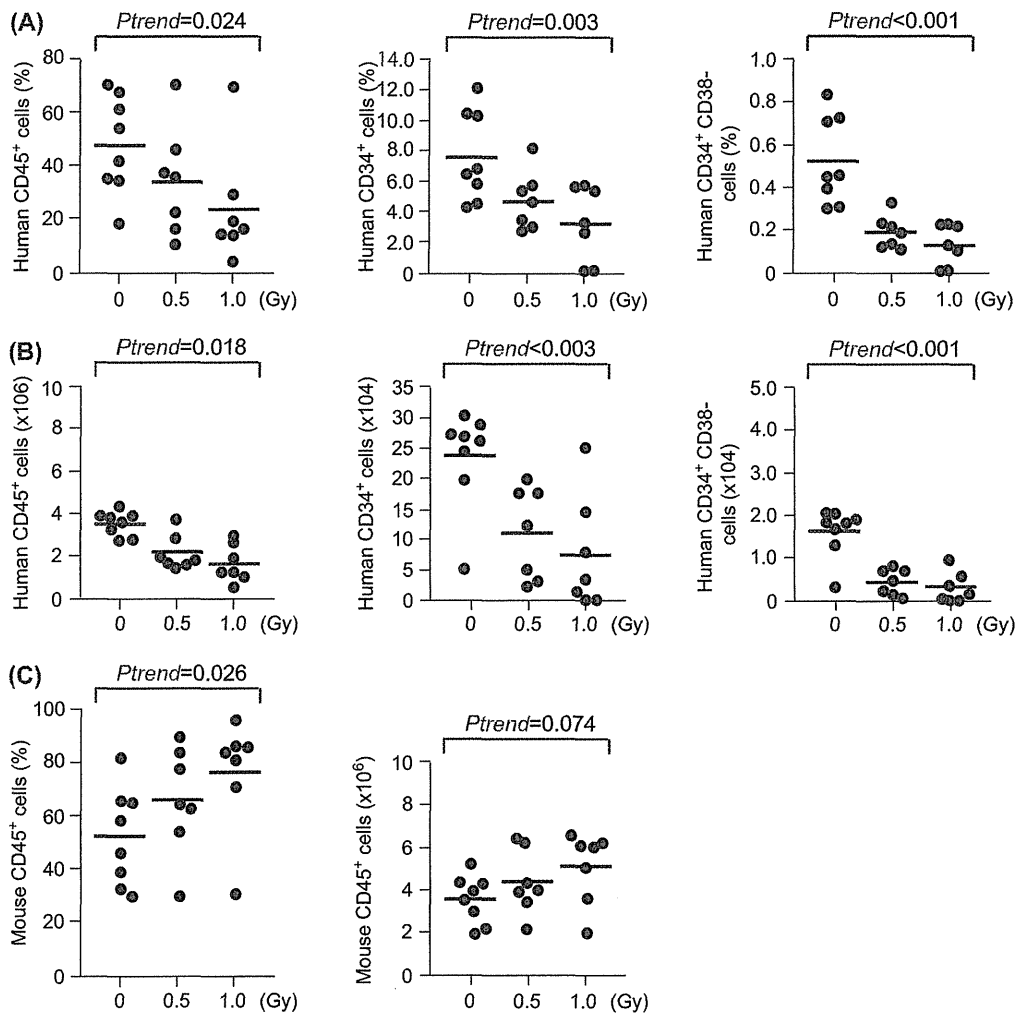


Figure 3. Contribution of human hematopoietic cells in BM of humanized mice following total-body irradiation (A) The chimerism of CD45⁺ human hematopoietic cells in BM mononuclear cells and percentages of CD34⁺ HSPC and CD34⁺CD38⁻ HSC in CD45⁺ human hematopoietic BM cells in NOG mice at the 12th week after irradiation. (B) The absolute numbers of CD45⁺ human hematopoietic cells, CD34⁺ HSPC and CD34⁺CD38⁻ HSC in BM (bilateral femurs and tibiae) of NOG mice at the 12th week after irradiation. (C) The chimerism of CD45⁺ mouse hematopoietic cells in BM mononuclear cells and the absolute numbers of CD45⁺ mouse hematopoietic cells in BM (bilateral femurs and tibiae) of NOG mice at the 12th week after irradiation.

in the humanized NOG mice, we used CD34⁺ HSPC which existed at the frequency 20-fold more than HSC for detection of $p16^{INK4A}$. Of note, expression of $p16^{INK4A}$ was detected only in HSPC from irradiated mice (Figure 4B).

Discussion

In this study, we demonstrated that the contribution of human cells to hematopoiesis in NOG mice declined in an X-ray dose-dependent manner at the 12th week after irradiation. This was in sharp contrast to an expectation that, following radiation exposure, highly-radiosensitive NOG mouse cells would be more seriously damaged than normal human cells. Decremental human hematopoiesis found in irradiated humanized mice was possibly caused by radiation dose-dependent decreases in the ability of transplanted and irradiated human HSC to repopulate following radiation injury. Indeed, increases in DNA damage

and $p16^{INK4A}$ expression were observed in human HSPC of irradiated humanized mice, potentially leading to a diminished proliferation ability of human HSPC in the irradiated hosts. Although higher levels of DNA damage were supposed to induce higher levels of $p16^{INK4A}$, the level of $p16^{INK4A}$ in human HSPC from humanized mice irradiated with 0.5 Gy appeared to be higher than that from mice with 1.0 Gy. Because excessive $p16^{INK4A}$ causes cellular senescence or apoptosis, more HSPC might be depleted in mice that received a higher dose of X-ray. However, this study could not address this issue, due to a small sample size lacking statistical power for association analysis. Further investigations with a robust study design will be necessary to fully evaluate associations of $p16^{INK4A}$ levels with DNA damage, radiation dose and hematopoietic ability of human HSC.

It is known that HSC suffer from various stresses, including replicative and oxidative stresses, during serial transplantation and eventually lose self-renewal capacity (Ito et al.

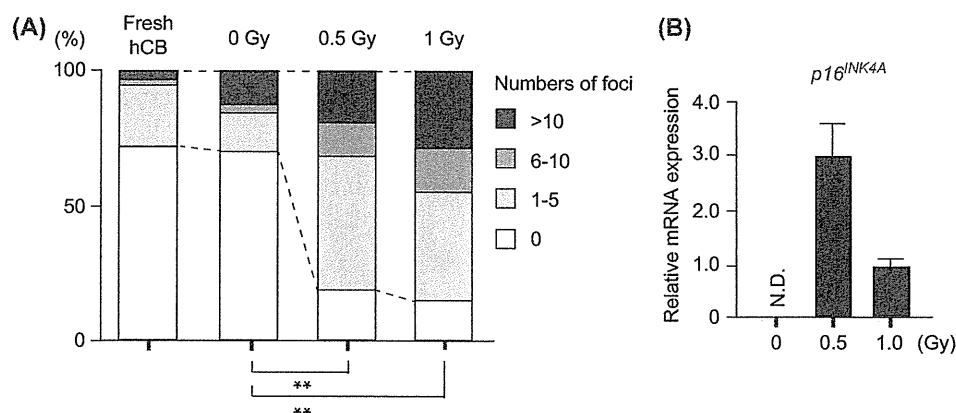


Figure 4. DNA damage and $p16^{INK4A}$ expression in human HSC of irradiated humanized mice (A) DNA damage response of $CD34^+CD38^-$ HSC at the 12th week after irradiation. BM cells from the humanized mice irradiated with doses indicated (0, 0.5, and 1.0 Gy) were pooled for each dose group. $CD34^+CD38^-$ human HSC were then purified by cell sorting from the pooled BM cells and stained with anti- γ H2AX. $CD34^+CD38^-$ HSC freshly isolated from hCB cells (Fresh hCB) were used as controls. Percentages of $CD34^+CD38^-$ HSC with indicated numbers of γ H2AX foci are depicted. Counting of 40 cells was repeated three times in each dose group. $**P < 0.001$ ($\chi^2 = 110.38$, $df = 6$). (B) Quantitative RT-PCR analysis of $p16^{INK4A}$ in $CD34^+$ human HSPC from irradiated humanized mice. $CD34^+$ HSPC were purified by cell sorting as in (A). Relative expression levels of $p16^{INK4A}$ mRNA were adjusted in reference to $GAPDH$ mRNA expression levels and determined as a ratio to the expression level in the cells from NOG mice irradiated with 1.0 Gy. Data are shown as the mean \pm SD for triplicate measurements. N.D. indicates not detected.

2006, Yahata et al. 2011). Serial transplantation of human HSC into immunodeficient mice triggers replicative stress that induces elevation of intracellular reactive oxygen species (ROS) levels along with the accumulation of persistent DNA damage within human HSC (Yahata et al. 2011). Thus, in our humanized mouse model, replicative and oxidative stresses caused by transplantation are likely to be augmented by radiation-induced DNA damage in transplanted human HSC. Restoration of HSC following marrow ablation is thought to highly rely on exogenous signals from the stem cell 'niche'. It has been reported that human and mouse HSC behave differently upon DNA damage following low-dose irradiation, i.e., DNA-damaged human HSC are prone to apoptosis and cannot well survive (Milyavsky et al. 2010) while similarly damaged mouse HSC tend to stay alive with competent DNA repair processes (Mohrin et al. 2010). However, there are considerable problems in terms of cross-reactivity of mouse molecules to human HSC, including cytokines, growth factors, and adhesion molecules. Furthermore, the NOG mice lack various immune cells, including T, B, and NK cells, that would normally be involved in producing supportive factors for HSC (Ito et al. 2002). In irradiated humanized mice, the mouse BM niche might provide less efficient survival signals for damaged human cells than for damaged mouse cells, and human hematopoiesis might become more compromised than mouse hematopoiesis. It is important to evaluate the consequence of DNA damage following irradiation in both human and mouse HSC in the same condition of BM niches. To this end, it would be challenging but may help to transplant human niche cells such as mesenchymal stem cells and/or stromal cells along with human HSC, or to use immunodeficient mice genetically engineered to express human cytokines such as stem cell factor and thrombopoietin (Rongvaux et al. 2011, Takagi et al. 2012).

The humanized mouse model in this study allowed us to assess the long-term radiation effects, including DNA

damage, at doses of 0.5 and 1.0 Gy on human HSC residing in the BM microenvironment. We propose that humanized mice should be able to serve as a valuable tool for risk assessment after radiation exposure and also for evaluating efficacy of preventive and therapeutic agents.

Acknowledgements

We thank Makiko Yui for technical assistance.

Declaration of interest

The authors report no conflicts of interest. The authors alone are responsible for the content and writing of the paper.

This work was supported in part by the U.S. National Institute of Allergy and Infectious Diseases (NIAID Contract HHSN272200900059C). The views of the authors do not necessarily reflect those of the two governments.

The Radiation Effects Research Foundation (RERF), Hiroshima and Nagasaki, Japan, is a private, nonprofit foundation funded by the Japanese Ministry of Health, Labor, and Welfare and the U.S. Department of Energy, the latter in part through DOE Award DE-HS0000031 to the National Academy of Sciences.

References

- Fulop GM, Phillips RA. 1990. The scid mutation in mice causes a general defect in DNA repair. *Nature* 347:479-482.
- Hamasaki K, Imai K, Hayashi T, Nakachi K, Kusunoki Y. 2007. Radiation sensitivity and genomic instability in the hematopoietic system: Frequencies of micronucleated reticulocytes in whole-body X-irradiated BALB/c and C57BL/6 mice. *Cancer Science* 98: 1840-1844.
- Ito K, Hirao A, Arai F, Takubo K, Matsuoka S, Miyamoto K, Ohmura M, Naka K, Hosokawa K, Ikeda Y, Suda T. 2006. Reactive oxygen species act through p38 MAPK to limit the lifespan of hematopoietic stem cells. *Nature Medicine* 12:446-451.

- Ito M, Hiramatsu H, Kobayashi K, Suzue K, Kawahata M, Hioki K, Ueyama Y, Koyanagi Y, Sugamura K, Tsuji K, Heike T, Nakahata T. 2002. NOD/SCID/gamma (c) (null) mouse: An excellent recipient mouse model for engraftment of human cells. *Blood* 100:3175-3182.
- Janzen V, Forkert R, Fleming HE, Saito Y, Waring MT, Dombkowski DM, Cheng T, DePinho RA, Sharpless NE, Scadden DT. 2006. Stem-cell ageing modified by the cyclin-dependent kinase inhibitor p16INK4a. *Nature* 443:421-426.
- Kyoizumi S, McCune J M, Namikawa R. 1994. Direct evaluation of radiation damage in human hematopoietic progenitor cells *in vivo*. *Radiation Research* 137:76-83.
- Milyavsky M, Gan OI, Trotter M, Komosa M, Tabach O, Notta F, Lechman E, Hermans KG, Eppert K, Kononova Z, Ornatsky O, Domany E, Meyn MS, Dick JE. 2010. A distinctive DNA damage response in human hematopoietic stem cells reveals an apoptosis-independent role for p53 in self-renewal. *Cell Stem Cell* 7:186-197.
- Mohrin M, Bourke E, Alexander D, Warr MR, Barry-Holson K, Le Beau MM, Morrison CG, Passegué E. 2010. Hematopoietic stem cell quiescence promotes error-prone DNA repair and mutagenesis. *Cell Stem Cell* 7:174-185.
- Nakachi K, Hayashi T, Hamatani K, Eguchi H, Kusunoki Y. 2008. Sixty years of follow-up of Hiroshima and Nagasaki survivors: Current progress in molecular epidemiology studies. *Mutation Research* 659:109-117.
- Rongvaux A, Willinger T, Takizawa H, Rathinam C, Auerbach W, Murphy AJ, Valenzuela DM, Yancopoulos GD, Eynon EE, Stevens S, Manz MG, Flavell RA. 2011. Human thrombopoietin knockin mice efficiently support human hematopoiesis *in vivo*. *Proceedings of the National Academy of Sciences of the USA* 108:2378-2383.
- Rossi DJ, Jamieson CH, Weissman IL. 2008. Stems cells and the pathways to aging and cancer. *Cell* 132:681-696.
- Rübe CE, Fricke A, Widmann TA, Fürst T, Madry H, Pfreundschuh M, Rübe C. 2011. Accumulation of DNA damage in hematopoietic stem and progenitor cells during human aging. *PLoS One* 6:e17487.
- Srivastava N, Gochhait S, De Boer P, Bamezai RN. 2009. Role of H2AX in DNA damage response and human cancers. *Mutation Research* 681:180-188.
- Takagi S, Saito Y, Hijikata A, Tanaka S, Watanabe T, Hasegawa T, Mochizuki S, Kunisawa J, Kiyono H, Koseki H, Ohara O, Saito T, Taniguchi S, Shultz LD, Ishikawa F. 2012. Membrane-bound human SCF/KL promotes *in vivo* human hematopoietic engraftment and myeloid differentiation. *Blood* 119:2768-2777.
- Wang Y, Schulte BA, LaRue AC, Ogawa M, Zhou D. 2006. Total body irradiation selectively induces murine hematopoietic stem cell senescence. *Blood* 107:358-366.
- Watson GE, Pocock DA, Papworth D, Lorimore SA, Wright EG. 2001. *In vivo* chromosomal instability and transmissible aberrations in the progeny of haemopoietic stem cells induced by high- and low-LET radiations. *International Journal of Radiation Biology* 77:409-417.
- Yahata T, Takanashi T, Muguruma Y, Ibrahim AA, Matsuzawa H, Uno T, Sheng Y, Onizuka M, Ito M, Kato S, Ando K. 2011. Accumulation of oxidative DNA damage restricts the self-renewal capacity of human hematopoietic stem cells. *Blood* 118:2941-2950.

Original Article

Improved PCR amplification for molecular analysis using DNA from long-term preserved formalin-fixed, paraffin-embedded lung cancer tissue specimens

Masataka Taga^{1*}, Hidetaka Eguchi^{1,2*}, Tomoko Shinohara¹, Keiko Takahashi¹, Reiko Ito¹, Wataru Yasui³, Kei Nakachi⁴, Yoichiro Kusunoki¹, Kiyohiro Hamatani¹

¹Department of Radiobiology/Molecular Epidemiology, Radiation Effects Research Foundation; ²Present address: Research Institute for Development Therapeutics & Translational Research Center, International Medical Center, Saitama Medical University; ³Department of Molecular Pathology, Hiroshima University Graduate School of Biomedical Sciences, Hiroshima, Japan. *These authors contributed equally to this work.

Received September 13, 2012; Accepted October 26, 2012; Epub November 20, 2012; Published January 1, 2013

Abstract: Archival tissue specimens are valuable resources of materials for molecular biological analyses in retrospective studies, especially for rare diseases or those associated with exposure to uncommon environmental events. Although successful amplification with PCR is essential for analysis of DNA extracted from archival formalin-fixed, paraffin-embedded (FFPE) tissue specimens, we have often encountered problems with poor PCR amplification of target fragments. To overcome this, we examined whether heat treatment in alkaline solution could efficiently restore the PCR template activity of DNA that had already been extracted from FFPE lung cancer tissue specimens. The effect of the heat treatment was assessed by PCR for the *TP53* gene and other lung cancer-related gene loci. The heat treatment of DNA samples in borate buffer resulted in successful PCR amplification of DNA fragments ranging from 91 to 152 bp. This technique for restoration of template activity of DNA for PCR amplification is very simple and economical, and requires no special apparatus, so it may be applicable for molecular analysis of DNA samples from FFPE tissue specimens at various laboratories.

Keywords: FFPE, lung tissue specimen, DNA restoration, PCR

Introduction

Radiation Effects Research Foundation (RERF) has collected and stored a large number of archival formalin-fixed, paraffin-embedded (FFPE) tissue specimens obtained from atomic bomb (A-bomb) survivors. Archival tissue specimens have become valuable, especially for histological and molecular biological analyses of radiation-associated cancers in the case of RERF. Most of these specimens were fixed with formalin, embedded in paraffin and stored at room temperature, and DNA extracted from such specimens has been used as templates for PCR amplification. However, we have often had problems with poor PCR amplification, i.e., insufficient amounts of DNA functioned as template compared with intact DNA, and the limitations in amplifiable DNA size [1]. These issues can be attributable at least in part to DNA frag-

mentation and chemical modifications caused by fixation in formalin [2].

Recently, improvements of DNA isolation from FFPE tissue specimens were reported on the basis of the antigen retrieval principle [3, 4]. FFPE tissue specimens, without deparaffinization, were incubated in alkaline buffer at high temperatures (80-120°C) for 20 min, followed by phenol/chloroform treatment and ethanol precipitation, which resulted in higher yields and better quality of DNA in terms of PCR amplification. The key mechanism of action of heating in alkaline solution for DNA may be to denature and hydrolyze proteins, resulting in 1) rupture of cell and nuclear membranes and 2) breakage of cross-linkages caused by formalin fixation [3].

It was also reported that the chemical modification of bases of RNA by fixation in formalin can

Preheating archival DNA for PCR amplification

Table 1. List of primers and PCR conditions

Gene or marker	Region	Primer sequence (5' -3')	Annealing temperature (°C)	Mg ²⁺ concentration (mM)	Extension temperature (°C)	Primer concentration (nM)	Size (bp)
TP53 (exon 8)	17p13	TGAGTAGTGGTA- ATCTACTGG TTGCTTACCTC- GCTTAGTGC	55	3 as MgCl ₂	72	200	152
TP53 (exon 7)	17p13	AGGTTGGCTCT- GACTGTACC CTCCTGACCTG- GAGTCTCC	55	3 as MgCl ₂	72	200	120
D3S1266 (for RARB)	3p22-24	ACCTT- TATGGGAGT- GTCCTTTGGGAGA TGGATG- GAAAANACGTAT- GTGTCTGTG	60	4 as MgSO ₄	68	250	112
D3S4614/Luca8.2 (for RASSF1)	3p21.3	GCTGAGAAATCT- CAATGTGGGTG GGCTGCTGAG- CAGTGTGAGAC	58	3 as MgCl ₂	72	500	126
D3S4103 (for FHIT)	3p14.2	GCAGAG- CAAGACCCTATCT- CAT TGCCTTGGGTAG- ATTATACCTG	60	2.5 as MgSO ₄	68	500	91
D9S171 (for CDKN2A)	9p21	CTCATCTCTGTCT- GCTGCCTCCT TTCTTGGGTC- TACTTTATTA- CAATCA	59	3.5 as MgSO ₄	68	250	109

be partially removed by incubation in TE buffer (pH 7.0) [5] or citrate buffer (pH 4.0) [6] at 70°C, resulting in restoration of template activity for RT-PCR. Based on the notion that heat treatment in alkaline buffer can be usable for DNA already extracted from FFPE tissue specimens in order to restore template activity for PCR, we examined whether heat treatment of DNA which had already been extracted from FFPE lung cancer tissue specimens in alkaline solution could efficiently restore PCR amplification.

Materials and methods

Tissue specimens and DNA extraction

Subjects of this study comprised 11 lung cancer cases found in a Life Span Study cohort of A-bomb survivors. FFPE lung cancer tissue specimens from subjects who had undergone surgery at local hospitals in Hiroshima during 1987 - 2001 were obtained and unlikably anonymized through the Study Group on Atomic Bomb Diseases, entrusted by the Ministry of Health, Labor and Welfare (MHLW) of Japan [7].

After deparaffinization of 5 µm sections using Hemo-De (Falma, Tokyo, Japan), the sections were stained with methylgreen (Sigma-Aldrich, St. Louis, MO) and dissected manually or by laser microdissection system AS LMD (Leica, Wetzlar, Germany). DNA was extracted from microdissected tissue sections using QIAamp DNA Micro kit (QIAGEN, Hilden, Germany), according to the manufacturer's instruction.

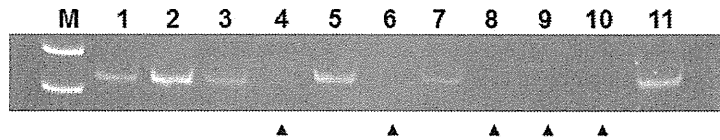
This study was conducted under approval of the Genetic and Medical Ethics Commission at Hiroshima University, and the Human Investigation Committee and the Ethics Committee for Genome Research at RERF.

Heat treatment of DNA in borate buffer and PCR

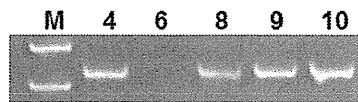
Four hundred ng of DNA was heated in 100 µl of 25 mM citrate-acetate buffer (pH 5.0 or 6.0), 25 mM Tris-HCl buffer (pH 7.0 or 8.0) or 25 mM borate-NaOH buffer (pH 9.0, 10.0, or 11.0) at various temperatures (25-120°C) for 30 min, followed by ethanol precipitation in the pres-

Preheating archival DNA for PCR amplification

A Before DNA restoration



B After DNA restoration



C

Case #	Duration of storage (yrs)	PCR for					
		TP53 (exon 8)	TP53 (exon 7)	D3S1266	D3S4614	D3S4103	D9S171
1*	14						
2*	15						
3*	18						
4	18						
5	17						
6	15						
7*	13						
8	12						
9	7						
10	4						
11*	4						

Figure 1. Improved PCR amplification by heating archival FFPE lung cancer tissue DNA in borate buffer. A: Polyacrylamide gel electrophoresis of PCR products (152 bp) for *TP53* (exon 8) using 10 ng of non-preheated DNA. Lane M is molecular size marker. Lanes 1-11 indicate PCR products of each lung cancer case. Closed arrow heads indicate cases with non-amplified DNA. B: PCR products amplified with 10 ng of preheated DNA. C: Summary of PCR amplification for *TP53* and lung cancer associated gene loci using non-preheated and preheated DNA. Empty grid indicates successful PCR using non-preheated DNA (in this case, PCR amplification using preheated DNA was not performed). Gray grid indicates successful PCR amplification using only preheated DNA. Black grid indicates no PCR amplification using either non-preheated or preheated DNAs. Cases with asterisks indicate successful PCR amplifications of all target fragments using 10 ng of non-preheated DNA.

ence of Ethachinmate (Nippon Gene, Tokyo, Japan) as carrier. Then, DNA was dissolved in TE buffer. As for PCR template, 10 ng of non-preheated or preheated DNA was used. PCR was performed using 0.5 U of Expand High Fidelity enzyme mixture (Roche Diagnostics, Basel, Switzerland) for *TP53*, 1 U of Platinum *Taq* DNA polymerase (Invitrogen, Carlsbad, CA) for D3S4614/Luca8.2, and 1 U of Platinum *Taq* DNA polymerase High Fidelity (Invitrogen) for D3S1266, D3S4103, and D9S171 in volume of 20 μ l containing 1 x PCR buffer, 200-400 μ M each of deoxyribonucleotide triphosphate mixture, Mg^{2+} , and each primer. PCR conditions consisted of initial denaturation (95°C for 2-3

min), followed by 44 cycles (40 cycles for *TP53*) of denaturation at 94°C for 30 sec, annealing for 1 min, extension for 30-60 sec, and a final extension for 7 min. Primer sets, temperatures of annealing and extension, and concentrations of Mg^{2+} are summarized in **Table 1**.

Results and discussion

Degraded DNA prepared from a colorectal cancer cell line, Colo210, that had been fixed with 15% unbuffered formalin for 3 days prior to DNA preparation, was used to preliminarily determine optimal conditions for heat treatment of DNA. As a result, preheating DNA to

Preheating archival DNA for PCR amplification

100 or 120°C in buffer with pH 11 was most effective for PCR amplification (data not shown). To assess the effect of preheating DNA extracted from FFPE lung cancer tissue specimens on PCR amplification, DNA was incubated in borate buffer (pH 11.0) at 100°C for 30 min. PCR amplification of exon 8 in the *TP53* gene with 10 ng of preheated DNA indicated that the treatment had restored DNA template activity for PCR amplification in 4 of 5 samples (Figure 1A and 1B). Similar effects were observed in PCR amplification of several lung cancer-associated gene loci, summarized in Figure 1C. However, one case (#6) showed no effects of heat treatment on most of its PCR amplifications, possibly because conditions for fixation and/or storage of the tissue specimen were so severe that preheat treatment could not restore template activity of DNA. Furthermore, in two FFPE thyroid tissue specimens stored at RERF, PCR amplification of *TP53* with only 2.5 ng of preheated DNA produced DNA fragments longer than 200 bp, while 25 ng of non-preheated DNA was required for the same PCR amplification (data not shown).

These observations suggest that heat-treatment either during DNA extraction or after DNA extraction can restore DNA template activity for PCR amplification, although the extent of restoration depends on conditions of fixation and storage of tissue specimens. This improvement of PCR amplification may be due to the partial elimination of chemical modification of nucleic acids generated by fixation with formalin, as seen in heat-treatment of RNA from FFPE tissue specimens [5, 6].

This technique is very simple, cost-saving, and requires no special apparatus. We think it will be applicable for various molecular analyses of DNA samples from long-term preserved FFPE tissue specimens in general.

Acknowledgments

The Radiation Effects Research Foundation (RERF), Hiroshima and Nagasaki, Japan is a private, non-profit foundation funded by the Japanese Ministry of Health, Labour and Welfare (MHLW) and the U.S. Department of Energy (DOE), the latter in part through DOE Award DE-HS0000031 to the National Academy of Sciences. This publication was supported by RERF Research Protocols B35-04 and B37-04,

and by JSPS Grant-in-Aid for Young Scientists (B) (21791238). The views of the authors do not necessarily reflect those of the two governments.

Conflict of interest statement

The authors have no conflicts of interest to disclose.

Address correspondence to: Dr. Masataka Taga, Department of Radiobiology/Molecular Epidemiology, Radiation Effects Research Foundation, 5-2 Hijiyama Park, Minami-ku, Hiroshima 732-0815, Japan. Tel: +81-82-261-3131; Fax: +81-82-261-3170; E-mail: taga@rerf.or.jp

References

- [1] Iwamoto KS, Mizuno T, Ito T, Akiyama M, Takeichi N, Mabuchi K and Seyama T. Feasibility of using decades-old archival tissues in molecular oncology/epidemiology. *Am J Pathol* 1996; 149: 399-406.
- [2] Srinivasan M, Sedmak D and Jewell S. Effect of fixatives and tissue processing on the content and integrity of nucleic acids. *Am J Pathol* 2002; 161: 1961-1971.
- [3] Shi SR, Cote RJ, Wu L, Liu C, Datar R, Shi Y, Liu D, Lim H and Taylor CR. DNA extraction from archival formalin-fixed, paraffin-embedded tissue sections based on the antigen retrieval principle: heating under the influence of pH. *J Histochem Cytochem* 2002; 50: 1005-1011.
- [4] Shi SR, Datar R, Liu C, Wu L, Zhang Z, Cote RJ and Taylor CR. DNA extraction from archival formalin-fixed, paraffin-embedded tissues: heat-induced retrieval in alkaline solution. *Histochem Cell Biol* 2004; 122: 211-218.
- [5] Masuda N, Ohnishi T, Kawamoto S, Monden M and Okubo K. Analysis of chemical modification of RNA from formalin-fixed samples and optimization of molecular biology applications for such samples. *Nucleic Acids Res* 1999; 27: 4436-4443.
- [6] Hamatani K, Eguchi H, Takahashi K, Koyama K, Mukai M, Ito R, Taga M, Yasui W and Nakachi K. Improved RT-PCR amplification for molecular analyses with long-term preserved formalin-fixed, paraffin-embedded tissue specimens. *J Histochem Cytochem* 2006; 54: 773-780.
- [7] Yasui W and Oue N. Systematic collection of tissue specimens and molecular pathological analysis of newly diagnosed solid cancers among atomic bomb survivors. In: Shibata Y, Namba H, Suzuki K, Tomonaga M, editors. *Radiation Risk Perspectives*. Amsterdam: Elsevier. 2007. pp: 81-86.

Rearranged Anaplastic Lymphoma Kinase (*ALK*) Gene in Adult-Onset Papillary Thyroid Cancer Amongst Atomic Bomb Survivors

Kiyohiro Hamatani,¹ Mayumi Mukai,¹ Keiko Takahashi,¹ Yuzo Hayashi,² Kei Nakachi,¹ and Yoichiro Kusunoki¹

Background: We previously noted that among atomic bomb survivors (ABS), the relative frequency of cases of adult papillary thyroid cancer (PTC) with chromosomal rearrangements (mainly *RET/PTC*) was significantly greater in those with relatively higher radiation exposure than those with lower radiation exposure. In contrast, the frequency of PTC cases with point mutations (mainly *BRAF*^{V600E}) was significantly lower in patients with relatively higher radiation exposure than those with lower radiation exposure. We also found that among ABS, the frequency of PTC cases with no detectable gene alterations in *RET*, neurotrophic tyrosine kinase receptor 1 (*NTRK1*), *BRAF*, or *RAS* was significantly higher in patients with relatively higher radiation exposure than those with lower radiation exposure. However, in ABS with PTC, the relationship between the presence of the anaplastic lymphoma kinase (*ALK*) gene fused with other gene partners and radiation exposure has received little study. In this study, we tested the hypothesis that the relative frequency of rearranged *ALK* in ABS with PTC, and with no detectable gene alterations in *RET*, *NTRK1*, *BRAF*, or *RAS*, would be greater in those having relatively higher radiation exposures.

Methods: The 105 subjects in the study were drawn from the Life Span Study cohort of ABS of Hiroshima and Nagasaki who were diagnosed with PTC between 1956 and 1993. Seventy-nine were exposed (>0 mGy), and 26 were not exposed to A-bomb radiation. In the 25 ABS with PTC, and with no detectable gene alterations in *RET*, *NTRK1*, *BRAF*, or *RAS*, we examined archival, formalin-fixed, paraffin-embedded PTC specimens for rearrangement of *ALK* using reverse transcription–polymerase chain reaction and 5′ rapid amplification of cDNA ends (5′ RACE).

Results: We found rearranged *ALK* in 10 of 19 radiation-exposed PTC cases, but none among 6 patients with PTC with no radiation exposure. In addition, solid/trabecular-like architecture in PTC was closely associated with *ALK* rearrangements, being observed in 6 of 10 PTC cases with *ALK* rearrangements versus 2 of 15 cases with no *ALK* rearrangements. The six radiation-exposed cases of PTC harboring both *ALK* rearrangements and solid/trabecular-like architecture were associated with higher radiation doses and younger ages at the time of the A-bombing and at diagnosis compared to the other 19 PTC with no detectable gene alterations.

Conclusion: Our findings suggest that *ALK* rearrangements are involved in the development of radiation-induced adult-onset PTC.

Introduction

THYROID CANCER IS ONE OF THE MALIGNANCIES most closely associated with exposure to ionizing radiation in humans (1), such as the atomic bombs in Hiroshima and Nagasaki and the Chernobyl nuclear power plant accident (2,3). Radiation Effects Research Foundation (RERF) epidemiology studies of atomic bomb survivors (ABS) have found that an

excess relative risk for papillary thyroid cancer (PTC) per Gy is remarkably high among survivors (4,5). The data from the studies after the Chernobyl accident also indicate a strong relationship between thyroid cancer and radiation exposure (3).

Gene alterations that lead to constitutive activation of the mitogen-activated protein kinase (MAPK)-signaling pathway—such as alterations of *RET*, neurotrophic tyrosine kinase receptor 1 (*NTRK1*), *BRAF*, and *RAS* genes—are

¹Department of Radiobiology/Molecular Epidemiology, Radiation Effects Research Foundation, Hiroshima, Japan.

²Geriatric Health Service Facility Hidamari, Hiroshima, Japan.

frequently found in PTC (6–8). These gene alterations can be detected in >70% of PTC cases, so the constitutive activation of the MAPK-signaling pathway appears to be a major early event in papillary thyroid carcinogenesis.

Our molecular analysis on rearrangements of *RET*, *NTRK1*, and *BRAF* genes, and also point mutations of *BRAF* and *RAS* genes in adult-onset PTC cases from the Life Span Study (LSS) cohort of ABS, found that the relative frequency of PTC cases with *RET/PTC* or *NTRK1* rearrangements (mainly *RET/PTC*) in all available PTC cases was significantly increased with an increased radiation dose, whereas PTC cases with *BRAF* or *RAS* point mutations (mainly *BRAF*^{V600E}) were significantly decreased (9,10). Apart from those PTC cases with known gene alterations, we found that the relative frequency of PTC cases with so-called nondetected gene alterations (i.e., no alterations in the *RET*, *NTRK1*, *BRAF*, or *RAS* gene) tended to increase with an increased radiation dose. The prevalence of the selected PTC cases peaked between 1956 and 1962, and rapidly decreased thereafter (10).

We postulated that some of the cases of PTC among ABS for which we had been unable to find gene alterations might have gene alterations that had previously not been looked for. Therefore, we initiated further molecular analyses of these cases by determining if some of them had rearrangements of anaplastic lymphoma kinase (*ALK*).

The *ALK* gene was first identified as a fusion partner of nucleophosmin in anaplastic large-cell lymphoma (ALCL) with the t(2;5) chromosomal rearrangement (11,12). Translocation of *ALK* with multiple fusion partner genes was subsequently identified in ALCL as well as in other inflammatory myofibroblastic tumors (13). One novel type of *ALK* rearrangement was an echinoderm microtubule-associated protein-like 4 (*EML4*)-*ALK* fusion gene, which was recently detected in nonsmall-cell lung cancer (14). Numerous *EML4-ALK* fusion variants have been identified to date (15–18). The *EML4-ALK* fusion variants were also detected in breast and colon cancers (19), but to date, there has been no report on *ALK* rearrangements in thyroid cancer.

In this study, we report for the first time the finding that *ALK* rearrangement selectively occurred in radiation-exposed PTC cases that carried no known gene alterations, and that about half of the PTC cases with rearranged *ALK* developed solid/trabecular-like architecture in the cancer tissue. The PTC cases harboring both *ALK* rearrangements and solid/trabecular-like architecture were related to higher radiation doses and younger ages at the time of the bombings and at diagnosis compared to the other cases, implying a key role of *ALK* rearrangements in the development of radiation-induced thyroid cancer.

Methods

Study subjects and tissue specimens

The study subjects were 105 adults with PTC who were members of the LSS cohort of ABS of Hiroshima and Nagasaki diagnosed in selected hospitals in the two cities between 1956 and 1993. Of these, 79 were exposed (>0 mGy) and 26 were not exposed to A-bomb radiation. Of these 105 patients, 71 had been a part of our previous study on *RET/PTC* rearrangements (10). The 26 nonradiation-exposed subjects were either those with a radiation dose estimated to be 0 mGy or those who were not in the city of Hiroshima or Nagasaki at

the time of the bombing. Study subjects who were not in these cities at the time of the bombing were assigned to the non-exposed group in this study, consistent with our previous article (10). This study was conducted with approval of the Human Investigation Committee and the Ethics Committee for Genome Research at the RERF.

Histological examination

Examination of histology was done by one of the authors (Y.H.) according to histopathological typing established by the WHO (20). All study specimens were nonbuffered, formalin-fixed, and paraffin-embedded PTC tissue specimens surgically resected from 1956 to 1993. Since amounts of tissue materials were limited, histological examination was conducted on one hematoxylin and eosin-stained tissue section per case.

RNA preparation and cDNA synthesis

RNA was extracted from microdissected noncancer or cancer regions using the High Pure RNA Paraffin Kit (Roche Diagnostics GmbH), as described previously (21). Reverse transcription was performed with random primers (9-mer) using 100 ng total RNA as template, as described previously (21).

Reverse transcription–polymerase chain reaction

Reverse transcription–polymerase chain reaction (RT-PCR) was carried out with the Fast Start High Fidelity PCR system (Roche Diagnostics GmbH) for the *ALK* gene, with AccuSure DNA polymerase (BIOLINE) for the *EML4* (exon 13)/*ALK* (exon 20) fusion and with Phusion Hot Start II (New England BioLabs) for the *EML4* (exon 20)/*ALK* (exon 20) fusion, using primer sets shown in Supplementary Table S1 (Supplementary Data are available online at www.liebertpub.com/thy) and as previously described (22).

Screening of rearranged *ALK*

The primer sets were made against the *ALK* kinase domain (K region) and the region spanning the boundary of exons 19 and 20 of *ALK* (W region) as shown in Figure 1A. PCR amplifications, for the K region with cDNA derived from 10 ng of total RNA of in-house control PTC and for the W region with cDNA from 5 ng of the same total RNA, were conducted at 36 cycles and 40 cycles, respectively. These PCR amplifications were repeated four times. The K/W ratios of 1.9 at 40 cycles or 2.9 at 36 cycles were drawn from an average of four experiments plus 2 × the standard deviation as shown in Figure 1C. When the intensity ratio of the K region to W region after a 40-cycle RT-PCR amplification was >1.9 (Fig. 1B; samples II, III, and IV) based on the calculation shown in Figure 1C, samples were further analyzed by 36-cycle PCR amplification to determine whether the samples were positive for *ALK* rearrangements. We assumed that the samples with an intensity ratio >2.9 at 36-cycle PCR amplification were positive for *ALK* rearrangements (Fig. 1B; samples II, III, and IV). We used only the K/W ratio for screening, and intensities of individual amplified DNA fragments were not taken into account for screening the candidates. This screening was conducted only when clear and detectable K-region bands were observed in the first PCR products. Subsequently, cDNA fragments of

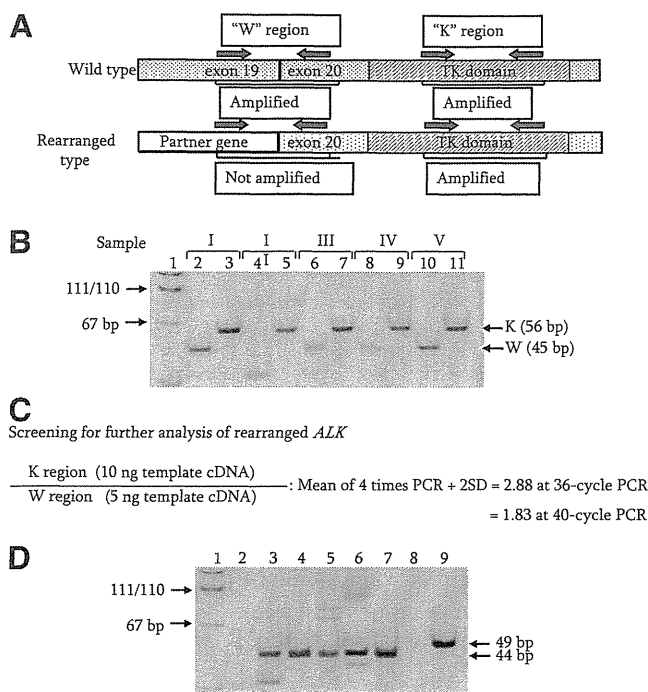


FIG. 1. (A) Diagram of the rearranged *ALK* gene. W and K regions indicate the regions spanning boundary of exons 19 and 20, and of exons 26 and 27 (kinase domain) in *ALK*, respectively. (B) Expression levels of W and K regions in *ALK*. The 5 μ L of 40-cycle PCR products were electrophoresed on an 8% acrylamide gel. Sample I (lanes 2 and 3) indicates RT-PCR products of in-house control PTC. Samples II–V (lanes 4–11) reveal RT-PCR products of four exposed PTC with nondetected gene alterations; lanes with even numbers are cDNA fragments derived from the W region, and those with odd numbers are fragments derived from the K region. Lane 1 indicates pUC19-*Msp*I digest for DNA size marker. (C) Screening of the rearranged *ALK* gene. The intensity ratio for selection of rearranged *ALK* was calculated using RT-PCR amplification with cDNA derived from 10 ng of total RNA of in-house control PTC for the K region, and with cDNA derived from 5 ng of total RNA of the same PTC for the W region as template. (D) Detection of expression of *EML4-ALK* fusion genes by RT-PCR. Lanes 3–7 indicate cDNA fragments of the *EML4-ALK* fusion gene in PTC cases from which the 3'-end fragments of exon 13 of *EML4* were isolated by the SMART RACE method. Lanes 6 and 7 correspond to PTC in samples IV and III of (B), respectively. Lane 9 indicates cDNA fragments (49 bp) derived from the chimera gene that was formed by fusion of exon 20 of *EML4* and exon 20 of *ALK*. Lanes 2 and 8 show H₂O for negative control, and Lane 1 shows pUC19-*Msp*I digest for DNA size marker. ALK, anaplastic lymphoma kinase; PTC, papillary thyroid cancer; RT-PCR, reverse transcription–polymerase chain reaction; RACE, rapid amplification of cDNA ends.

rearranged *ALK* genes were isolated and analyzed by the SMART rapid amplification of cDNA end (RACE) method, using primer sets shown in Supplementary Table S1 as described previously (22).

Statistical analysis

The Fisher's exact test was used for categorical variables. The Mann–Whitney *U* test was used for nonparametric two-sample comparison of continuous variables. SPSS software

(version 15.0) was used for the statistical analyses. *p*-value was calculated by using a two-sided test. The Cochran–Armitage test for nonparametric trend analysis was carried out with Excel Statistics 2006 software.

Radiation dose

A-bomb radiation dose used in the analyses were shielded-organ doses to the thyroid as estimated by the recently implemented DS02 system (23), except for those cohorts who were not in the city of Hiroshima or Nagasaki at the time of the bombing.

Results

Detection of *ALK* rearrangements in PTC cases with previously nondetected gene alterations

Molecular epidemiological characteristics of 105 PTC cases examined thus far are shown in Supplementary Table S2, with 34 PTC cases that were newly added after our previous article (10). When comparing 79 radiation-exposed subjects and 26 nonexposed ones, no significant differences were found in distribution of gender, city, age at the time of the bombing (ATB), age at diagnosis, or presence or absence of *RET/PTC* rearrangements, *NTRK1* rearrangements, and *BRAF* or *RAS* point mutations. However, relative frequencies of *RET/PTC* rearrangements and *BRAF* mutation in radiation-exposed PTC cases showed significantly increasing or decreasing trends depending on the radiation dose ($P_{\text{trend}}=0.01$ and 0.0006), as shown in Supplementary Table S2. Furthermore, when comparing nonexposed PTC cases with those exposed to relatively a high radiation dose (the 3rd tertile, >355 mGy) for *RET/PTC* rearrangements, the relative frequency was significantly higher in exposed PTC cases (>355 mGy) than in nonexposed PTC cases (1/26 cases vs. 9/26 cases, respectively; $p=0.01$). On the other hand, the relative frequency of the *BRAF* mutation was significantly lower in PTC cases exposed to the radiation dose (>355 mGy) than in nonexposed PTC cases (19/26 cases vs. 7/26 cases, respectively; $p=0.002$). Among 105 PTC cases examined thus far for *RET*, *NTRK1*, and *BRAF* rearrangements and *BRAF* and *RAS* point mutations, 25 PTC cases were found to have no alterations in these genes, which tended to increase with an increased radiation dose, though this is not statistically significant (Supplementary Table S2). It should be noted that these cases showed a temporal change with a peak a short time after exposure, which then rapidly decreased (i.e., median time after exposure was 23 years for this group vs. 32 years for cases with *BRAF* and *RAS* point mutations, $p=0.014$). These findings are consistent with those in our previous article (10).

Of 25 PTC cases with previously nondetected gene alterations (also referred to as nondetected gene alterations) that carried no alterations in *RET*, *NTRK1*, *BRAF*, or *RAS* genes, we found *ALK* rearrangements in 10 of 19 radiation-exposed cases, but no *ALK* rearrangements in any of the six nonexposed cases (Table 1). The median dose in PTC cases with rearranged *ALK* was significantly higher than in grouped radiation-exposed and nonradiation-exposed PTC cases with no rearranged *ALK* (Fig. 2). However, there was no significant difference in the radiation dose between radiation-exposed PTC cases with rearranged *ALK* and with non-rearranged *ALK*. SMART 5' RACE followed by sequencing analysis

TABLE 1. REARRANGED *ALK* IN PAPILLARY THYROID CANCER CASES WITH NONDETECTED GENE ALTERATIONS

PTC case	ALK rearrangements		p ^a
	Present	Absent	
Nonexposed (n=6)	0	6	0.051
Exposed (>0 mGy, n=19)	10 ^b	9	

^aFisher's exact test.

^bFive cases were *EML4*(exon 13)/*ALK*(exon 20); one case was *EML4*(exon 20)/*ALK*(exon 20); *ALK* partner genes in four cases have not been determined yet.

PTC, papillary thyroid cancer.

revealed that five PTC cases with rearranged *ALK* were a fusion of *EML4* (exon 13) and *ALK* (exon 20), and that one case was a fusion of *EML4* (exon 20) and *ALK* (exon 20) (Table 1). Expression of cDNA fragments of chimeric *EML4-ALK* in the PTC cases was confirmed by RT-PCR (Fig. 1D, lanes 3–7, and 9). The counterpart genes in the remaining four cases are currently being studied.

Morphological characteristics in PTC with rearranged *ALK*

Histological review of the 10 PTC cases with rearranged *ALK* found that 6 of the 10 had solid/trabecular-like architecture comprising either several small sites or several sites of greater total area within the cancer regions, but did not have insular architecture. Necrosis or mitotic figures were not observed in the single tissue section examined for each case. Supplementary Figure S1A and B show pathological photographs of two PTC cases with rearranged *ALK*, with solid/trabecular-like architecture in more than 50% of the cancers. Supplementary Figure S1C and D reveal a typical papillary

TABLE 2. ASSOCIATION BETWEEN REARRANGED *ALK* AND SOLID/TRABECULAR-LIKE ARCHITECTURE

	Rearranged <i>ALK</i>		p ^a
	Present (n=10)	Absent (n=15)	
Solid/trabecular-like architecture ^b			0.028
Present	6 ^c	2	
Absent	4	13	

Data represent 25 PTC cases with nondetected gene alterations.

^aFisher's exact test.

^bThe samples were counted as positive for solid/trabecular-like architecture when that architecture was found in several areas within cancer regions.

^cMore than 50% of cancer regions revealed such architecture in two cases.

structure for two exposed PTC cases with no rearranged *ALK*. In contrast, only 2 of 15 PTC cases with no rearranged *ALK* had such architecture. Analysis of 25 PTC cases with nondetected gene alterations revealed a close association between *ALK* rearrangement and solid/trabecular-like architecture ($p=0.028$, Table 2).

Association of PTC harboring both rearranged *ALK* and solid/trabecular-like architecture with radiation dose and age at A-bombing

Since there were only two PTC cases with no rearranged *ALK*, but having solid/trabecular-like architecture, we compared six PTC cases harboring both rearranged *ALK* and solid/trabecular-like architecture with the remaining 19 PTC cases in terms of radiation dose and ages at A-bombing and diagnosis (Fig. 3). These six PTC cases received significantly greater radiation doses and were or younger age at the time of A-bombing and at the time of diagnosis compared to the other 19 PTC cases (Fig. 3A–C, $p=0.005$, 0.008, and 0.016, respectively). Furthermore, comparison of 6 PTC cases harboring both rearranged *ALK* and solid/trabecular-like architecture with the remaining exposed 13 PTC cases by Mann–Whitney test also showed significant differences for radiation ($p=0.036$), age at A-bombing ($p=0.021$), and age at diagnosis ($p=0.020$).

Discussion

We report here the first evidence that rearrangements of *ALK* in adult-onset PTC cases develop in subjects exposed to radiation. Furthermore, the median radiation dose in PTC cases with rearranged *ALK* was significantly higher than in PTC cases with no rearranged *ALK* (Fig. 2), indicating involvement of rearranged *ALK* in radiation-induced papillary thyroid carcinogenesis. However, since only six nonexposed PTC cases were examined for rearranged *ALK*, it is necessary to examine a larger number of sporadic PTC cases to clarify possible presence of *ALK* rearrangements. We are thus unable at present to exclude the possibility that *ALK* rearrangements also occur in sporadic PTC. Although partner genes in four PTC cases have not yet been identified, PCR amplification in these cases was found in the K region, but not in the W region (Fig. 1), and therefore these PTC cases were judged to have rearranged *ALK*. We are attempting to identify the partner genes.

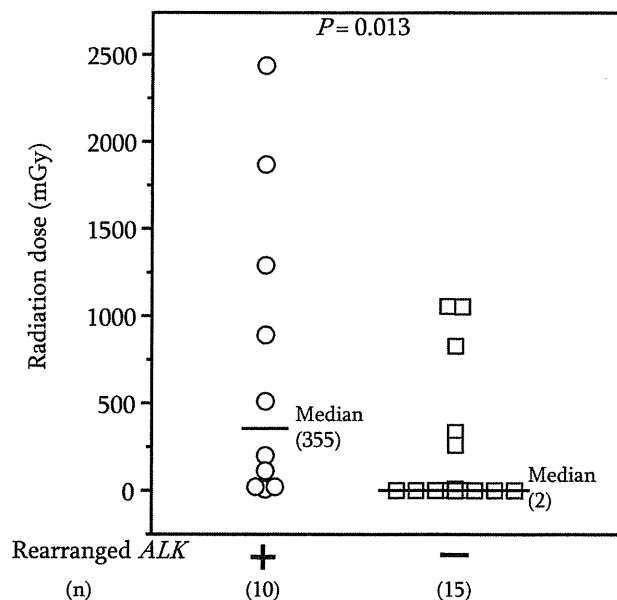


FIG. 2. Comparison of radiation dose distribution in PTC cases with (+, O) and without (-, □) rearranged *ALK*.

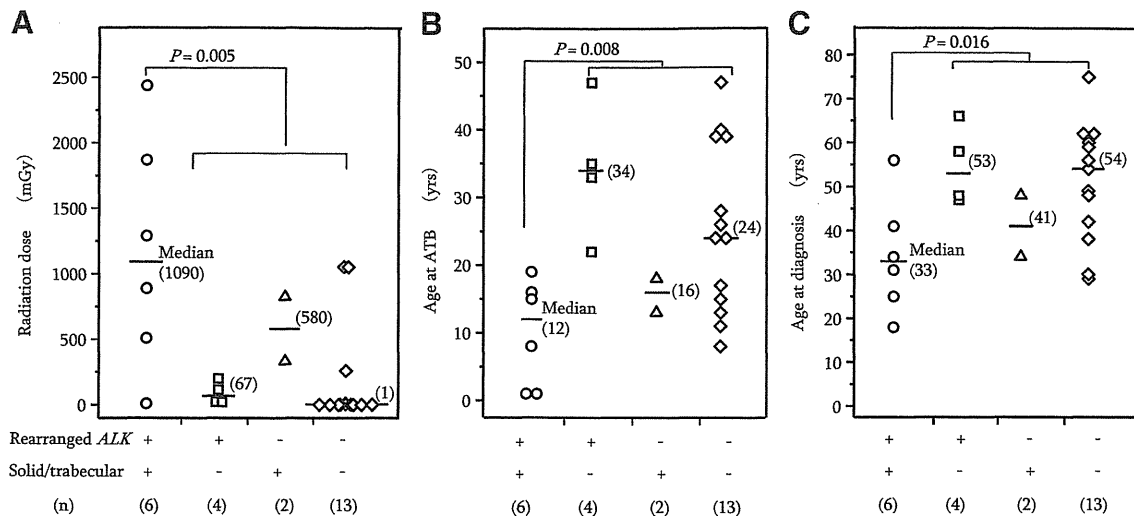


FIG. 3. Epidemiological characteristics of PTC cases harboring both the rearranged *ALK* gene and solid/trabecular-like architecture, in relation to radiation dose (A), age at the time of atomic bombing (B), and age at the time of diagnosis (C).

Some of the 10 PTC cases with rearranged *ALK* revealed weak, but observable, PCR-amplified fragments as shown in Figure 1C. Those bands may be in part due to amplified fragments derived from another allele with wild-type *ALK*. Another plausible interpretation is that the rearrangement did not occur in all tumor cells. It is important to clarify whether *ALK* rearrangement is a driver mutation or a passenger mutation to better understand radiation-related carcinogenesis of PTC. Furthermore, although rearrangements of *ALK* are involved in the pathogenesis of many malignancies, including lymphoma and lung cancer, few *ALK* rearrangements have been well defined relative to their pathogenic role in cancer. Recently, constitutive *ALK* activation in several cancers was reported to cause the activation of selected downstream pathways, including MAPK and STAT (24,25), but no reports are available regarding a putative pathogenic role of rearranged *ALK* in PTC. To assess biological significance of rearranged *ALK* in radiation-induced PTC, *in vitro* and *in vivo* comparative experiments with *RET/PTC* rearrangements and *BRAF* point mutation need to be performed to shed light on these issues.

The nonradiation-exposed subjects in this study were comprised of two distinct groups: subjects whose radiation dose levels were estimated to be zero by the DS02 system, and subjects who were not in Hiroshima or Nagasaki, and thus not a part of the DS02 dose estimation. Our analyses included two not-in-city subjects in the six nonexposed subjects with non-detected gene alterations, but even when we excluded these not-in-city subjects from the analysis, the results were substantially unchanged. Specifically, the six nonexposed subjects without rearranged *ALK* in Table 1 would become 4 ($p=0.1$ in this case); the median value of 2 mGy for 15 subjects with no rearranged *ALK* in Figure 2 would become 3 mGy for 13 subjects ($p=0.034$); and the 13 subjects (denoted by "◇") in Figure 3 harboring neither rearranged *ALK* nor solid/trabecular-like architecture would become 11, and their median values of 1 mGy, 24 years, and 54 years in Figure 3A–C would be 2 mGy, 24 years, and 54 years ($p=0.009$, 0.012, and 0.023), respectively.

The solid/trabecular-like architecture appeared in one of three different types of groupings as (I) relatively small, clonal, multicellular clusters distributed throughout the cancer; (II) larger groupings (each composed of a few multicellular clusters) distributed throughout the cancer, or as (III) a few large groupings that occupied a major portion (>50%) of the cancer volume. Interestingly, 6 of 10 PTC cases with rearranged *ALK* had solid/trabecular-like architecture corresponding to types (I) and (II) above (numbering 3 and 1, respectively) in several areas within the cancers, and two cases had such architecture in more than 50% of the cancer (type III and shown in Supplementary Fig. 1A, B). However, only 2 of 15 PTC cases with no rearranged *ALK* had such architecture; they were small and found in several areas scattered throughout the cancer (type I). The 25 PTC cases with nondetected gene alterations showed no necrosis or mitotic figures, but did show PTC-specific nuclear features such as nuclear grooves, intranuclear cytoplasmic inclusions, and psammoma bodies. Taking into account the diagnostic criteria proposed by Volante *et al.* (26), it is reasonable to conclude that two PTC cases harboring solid/trabecular-like architecture in more than 50% of cancer regions are a mixed type of PTC and solid variant, or a solid variant of PTC rather than poorly differentiated thyroid cancer. This is true even though the size of one solid/trabecular nest was small and uniform compared with that of post-Chernobyl childhood PTC, and that the other six PTC cases (four and two with and without rearranged *ALK*, respectively) harboring such architecture in several cancer regions are typical PTC.

PTC cases harboring both rearranged *ALK* and solid/trabecular-like architecture were significantly associated not only with a greater radiation dose but also with younger age at the time of bombing and at diagnosis, compared with the remaining PTC cases. One plausible interpretation of this finding is that in the process of radiation-induced papillary thyroid carcinogenesis involving *ALK* rearrangements, unknown gene alterations may additionally occur and generate solid/trabecular-like architecture. Considering this, further analysis will be required to identify such gene alterations and

to assess the pathogenic role of *ALK* rearrangements and its potential link to solid/trabecular-like architecture.

Acknowledgments

The RERF, Hiroshima and Nagasaki, Japan, is a private, nonprofit foundation funded by Japan's Ministry of Health, Labour, and Welfare, and the U.S. Department of Energy (DOE), the latter in part through DOE Award DE-HS0000031 to the National Academy of Sciences. This publication was supported by RERF Research Protocols RP 5-02, and in part by a Grant-in-Aid for Science Research from the Ministry of Education, Culture, Sports, Science, and Technology, and a Grant-in Aid for Cancer Research from Japan's Ministry of Health, Labour, and Welfare, as well as research grant for the Princess Takamatsu Cancer Research Fund (08-24015). We thank Dr. J. Cologne for his helpful statistical advice, Mr. K. Koyama for his excellent technical assistance, and Ms. M. Yonezawa for her good help with preparation of article. The views of the authors do not necessarily reflect those of the two governments.

Disclosure Statement

The authors declare that they have no commercial associations that might create a conflict of interest in connection with this article.

References

1. Imaizumi M, Usa T, Tominaga T, Neriishi K, Akahoshi M, Nakashima E, Ashizawa K, Hida A, Soda M, Fujiwara S, Yamada M, Ejima E, Yokoyama N, Okubo M, Sugino K, Suzuki G, Maeda R, Nagataki S, Eguchi K 2006 Radiation dose-relationships for thyroid nodules and autoimmune thyroid diseases in Hiroshima and Nagasaki atomic bomb survivors 55–58 years after radiation exposure. *JAMA* **295**: 1011–1022.
2. Kazakov VS, Demidchik EP, Astakhova LN 1992 Thyroid cancer after Chernobyl. *Nature* **359**:21.
3. Astakhova LN, Anspaugh LR, Beebe G.W, Bouville A, Drozdovitch VV, Garber V, Gavrillin YI, Khrouch VT, Kuvshinnikov AV, Kuzmenkov YN, Minenko VP, Moschik KV, Nalivko AS, Robbins J, Shemiakina EV, Shinkarev S, Tochitskaya SI, Waclawiw MA 1998 Chernobyl-related thyroid cancer in children of Belarus: A case-control study. *Radiat Res* **150**:349–356.
4. Thompson DE, Mabuchi K, Ron E, Soda M, Tokunaga M, Ochikubo S, Sugimoto S, Ikeda T, Terasaki M, Izumi S, Preston DL 1994 Cancer incidence in atomic bomb survivors. Part II: Solid tumors, 1958–1987. *Radiat Res* **137**:S17–S67.
5. Preston DL, Ron E, Tokuoka S, Funamoto S, Nishi N, Soda M, Mabuchi K, Kodama K 2007 Solid cancer incidence in atomic bomb survivors: 1958–1998. *Radiat Res* **168**:1–64.
6. Gandhi M, Evdokimova V, Nikiforov YE 2010 Mechanisms of chromosomal rearrangements in solid tumors: the model of papillary thyroid carcinoma. *Mol Cell Endocrinol* **321**:36–43.
7. Greco A, Miranda C, Pierotti MA 2010 Rearrangements of *NTRK1* gene in papillary thyroid carcinoma. *Mol Cell Endocrinol* **321**:44–49.
8. Xing M 2010 Prognostic utility of *BRAF* mutation in papillary thyroid cancer. *Mol Cell Endocrinol* **321**:86–93.
9. Takahashi K, Eguchi H, Arihiro K, Ito R, Koyama K, Soda M, Cologne J, Hayashi Y, Nakata Y, Nakachi K, Hamatani K 2007 The presence of *BRAF* point mutation in adult papillary thyroid carcinomas from atomic bomb survivors correlates with radiation dose. *Mol Carcinog* **46**:242–248.
10. Hamatani K, Eguchi E, Ito R, Mukai M, Takahashi K, Taga M, Imai K, Cologne J, Soda M, Arihiro K, Fujihara M, Abe K, Hayashi T, Nakashima M, Sekine I, Yasui W, Hayashi Y, Nakachi K 2008 *RET/PTC* rearrangements preferentially occurred in papillary thyroid cancer among atomic bomb survivors exposed to high radiation dose. *Cancer Res* **68**: 7176–7182.
11. Morris SW, Kirstein MN, Valentine MB, Dittmer KG, Shapiro DN, Saltman DL, Look AT 1994 Fusion of a kinase gene, *ALK*, to a nucleolar protein gene, *NPM*, in non-Hodgkin's lymphoma. *Science* **263**:1281–1284.
12. Shiota M, Fujimoto J, Tanegawa M, Satoh H, Ichinohasama R, Abe M, Nakano M, Yamamoto T, Mori S 1994 Diagnosis of t(2;5)(p23;q35)-associated Ki-1 lymphoma with immunohistochemistry. *Blood* **84**:3648–3652.
13. Pulford K, Morris SW, Turturro F 2004 Anaplastic lymphoma kinase proteins in growth control and cancer. *J Cell Physiol* **199**:330–358.
14. Soda M, Choi YL, Enomoto M, Takada S, Yamashita Y, Ishikawa S, Fujiwara S, Watanabe H, Kurashina K, Hatanaka H, Bando M, Ohno S, Ishikawa Y, Aburatani H, Niki T, Sohara Y, Sugiyama Y, Mano H 2007 Identification of the transforming *EML4-ALK* fusion gene in non-small-cell lung cancer. *Nature* **448**:561–566.
15. Mano H 2008 Non-solid oncogenes in solid tumors: *EML4-ALK* fusion genes in lung cancer. *Cancer Sci* **99**: 2349–2355.
16. Choi YL, Takeuchi K, Soda M, Inamura K, Togashi Y, Hatano S, Enomoto M, Hamada T, Haruta H, Watanabe H, Kurahashi K, Hatanaka H, Ueno T, Takada S, Yamashita Y, Sugiyama Y, Ishikawa Y, Mano H 2008 Identification of novel isoforms of the *EML4-ALK* transforming gene in non-small cell lung cancer. *Cancer Res* **68**:4971–4976.
17. Takeuchi K, Choi YL, Soda M, Inamura K, Togashi Y, Hatano S, Enomoto M, Takada S, Yamashita Y, Satoh Y, Okumura S, Nakagawa K, Ishikawa Y, Mano H 2008 Multiplex reverse transcription-PCR screening for *EML4-ALK* fusion transcripts. *Clin Cancer Res* **14**:6618–6624.
18. Takeuchi K, Choi YL, Togashi Y, Soda M, Hanata S, Inamura K, Takada S, Ueno T, Yamashita Y, Satoh Y, Okumura S, Nakagawa K, Ishikawa Y, Mano H 2009 KIF5B-*ALK*, a novel fusion oncokinas identified by an immunohistochemistry-based diagnostic system for *ALK*-positive lung cancer. *Clin Cancer Res* **15**:3143–3149.
19. Lin E, Li L, Guan Y, Soriano R, Rivers CS, Mohan S, Pandita A, Tang J, Modrusan Z 2009 Exon array profiling detects *EML4-ALK* fusion in breast, colorectal, and non-small cell lung cancers. *Mol Cancer Res* **7**:1466–1476.
20. DeLellis RA, Lloyd RV, Heitz PU, Eng C (eds) 2004 World Health Organization Classification of Tumours. Pathology and Genetics of Tumours of Endocrine Organs. IARC Press, Lyon, France.
21. Hamatani K, Eguchi H, Takahashi K, Koyama K, Mukai M, Ito R, Taga M, Yasui W, Nakachi K 2006 Improved RT-PCR amplification for molecular analyses with long-term preserved formalin-fixed, paraffin-embedded tissue specimens. *J Histochem Cytochem* **54**:773–780.
22. Hamatani K, Eguchi H, Mukai M, Koyama K, Taga M, Ito R, Hayashi Y, Nakachi K 2010 Improved methods for analysis of RNA present in long-term preserved thyroid cancer tissue of atomic bomb survivors. *Thyroid* **20**:43–49.

23. Young RW, Kerr GD (eds) 2005 Reassessment of the Atomic Bomb Radiation Dosimetry for Hiroshima and Nagasaki Dosimetry System 2002. Radiation Effects Research Foundation, Hiroshima, Japan.
24. Chiarle R, Voena C, Ambrogio C, Piva R, Inghirami G 2008 The anaplastic lymphoma kinase in the pathogenesis of cancer. *Nat Rev Cancer* 8:11–23.
25. Shaw ST, Solomon B 2011 Targeting anaplastic lymphoma kinase in lung cancer. *Clin Cancer Res* 17:2081–2086.
26. Volante M, Collini P, Nikiforov YE, Sakamoto A, Kakudo K, Katoh R, Lloyd RV, LiVolsi VA, Papotti M, Sobrinho-Simoes M, Bussolati G, Rosai J 2007 Poorly differentiated thyroid carcinoma: the Turin proposal for the use of uniform diagnostic criteria and an algorithmic diagnostic approach. *Am J Surg Pathol* 31:1256–1264.

Address correspondence to:

Kiyohiro Hamatani, Ph.D.

Department of Radiobiology/Molecular Epidemiology

Radiation Effects Research Foundation

5-2 Hijiyama Park

Minami-ku

Hiroshima 732-0815

Japan

E-mail: hamatani@rerf.or.jp